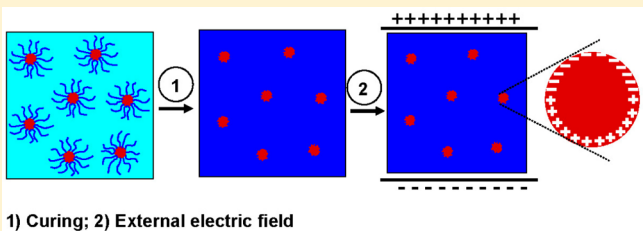


Dielectric Constant Enhancement of Epoxy Thermosets via Formation of Polyelectrolyte Nanophases

Houluo Cong, Jingang Li, Lei Li, and Sixun Zheng*

Department of Polymer Science and Engineering and the State Key Laboratory of Metal Matrix Composites, Shanghai Jiao Tong University, Shanghai 200240, P. R. China

ABSTRACT: Poly(ethylene oxide)-*b*-poly(sodium *p*-styrenesulfonate) (PEO-*b*-PSSNa) diblock copolymer was synthesized and then incorporated into epoxy to obtain the nanostructured epoxy thermosets containing polyelectrolyte nanophases. This PEO-*b*-PSSNa diblock copolymer was synthesized via the radical polymerization of *p*-styrenesulfonate mediated with 4-cyano-4-(thiobenzoylthio)valeric ester-terminated poly(ethylene oxide). The formation of polyelectrolyte (i.e., PSSNa) nanophases in epoxy followed a self-assembly mechanism. The precursors of epoxy acted as the selective solvent of the diblock copolymer, and thus, the self-assembled nanostructures were formed. The self-organized nanophases were fixed through the subsequent curing reaction. By means of transmission electron microscopy (TEM) and small-angle X-ray scattering (SAXS), the morphologies of the nanostructured epoxy thermosets containing PSSNa nanophases were investigated. In the glassy state, the epoxy matrixes were significantly reinforced by the spherical PSSNa nanodomains, as evidenced by dynamic mechanical analysis. The measurement of dielectric properties showed that, with the incorporation of PSSNa nanophases, the dielectric constants of the epoxy thermoset were significantly increased. Compared to the control epoxy, the dielectric loss of the nanostructured thermosets still remained at quite a low level, although the values of dielectric loss were slightly increased with inclusion of PSSNa nanophases.



1) Curing; 2) External electric field

INTRODUCTION

Epoxy are among the most important thermosetting polymers and have been widely applied as adhesives, coatings, and matrixes of composites due to their excellent chemical resistance and high mechanical strength.^{1–3} Owing to low temperature processability, mechanical flexibility, and compatibility with integrated circuit boards, epoxies are also the choice of the major electric encapsulation materials for embedded passives such as resistors, capacitors, and inductors.^{4,5} In some applications, such as high-speed digital circuits with high frequency, it is required that the insulating materials (e.g., epoxy) possess a low dielectric constant, which is favorable for the miniaturization and integration of the device, as well as a high information transfer rate, and crosstalk reduction.⁶ In other applications, however, the epoxy polymers with high dielectric constants are highly desired, which can facilitate electric charge storage, transportation, and heat dissipation in these materials.^{7,8} It is important to investigate and modulate the dielectric properties of epoxy polymers. It has been realized that the dielectric constants of epoxy thermosets can be increased by incorporating some conductive fillers such as metals (e.g., silver, aluminum, and nickel),^{9,10} ferroelectric ceramics,^{11,12} carbon nanotubes,^{13–17} and some conductive (or piezoelectric) polymers.^{18,19} Generally, a dramatic increase of dielectric constant can be attained before a percolation threshold of filler concentration is reached.^{20,21} In these composite systems, the fine dispersion of the fillers in epoxy thermosets is critical to fulfill the enhancement of dielectric constants. The types, sizes, and dispersion degrees of the fillers

can significantly affect the properties of the resulting composites. Polyelectrolytes are a class of important polymers bearing oppositely charged segments (i.e., both cationic and anionic repeat groups). It is anticipated that the dielectric constants of epoxy would be increased while polyelectrolytes are incorporated into epoxy matrix. However, simple physical blending of epoxy with polyelectrolyte is less effective and would cause macroscopic phase separation. The nanoscaled dispersion of conductive fillers in epoxy thermosets would significantly optimize the intercomponent interactions by creating a great amount of interface polarizable under external alternating current fields, and thus, the dielectrics of the materials are significantly enhanced.

It has been demonstrated that the nanophases in thermosets can be formed by incorporating amphiphilic block copolymers. Hillmyer et al.^{22,23} first reported that epoxy containing ordered spherical nanophases were accessed by the use of an amphiphilic block copolymer via a self-assembly approach. In this protocol, the precursors of epoxy acted as the selective solvent of the block copolymer and the self-assembled microdomains were formed. The preformed microphase-separated morphologies were locked in via a curing reaction. More recently, it is realized that ordered or disordered nanophases in thermosets can be alternatively obtained via the reaction-induced microphase separation (RIMPS) ap-

Received: September 4, 2014

Revised: November 22, 2014

Published: December 8, 2014

proach.^{24,25} In the RIMPS approach, it is not required that block copolymers are self-assembled into the nanophases in the precursors of the thermosets. The nanophases are not formed until the polymerization is carried out with the sufficiently high conversion of the precursors. In the past years, many investigators have reported the nanophases were formed in thermosets by using a variety of block copolymers via the self-assembly or RIMPS approach.^{26–55} In most of the previous reports, the main purpose was to investigate the correlation of the mechanical properties (e.g., fracture toughness) with the morphologies of the materials.^{2,56} To the best of our knowledge, there have been few reports on the improvement of the dielectric properties of the thermosets via the formation of polyelectrolyte nanophases by the use of a polyelectrolyte-subchain-containing amphiphilic block copolymer.

In this work, we explored incorporating polyelectrolyte nanophases into epoxy by using a polyelectrolyte-subchain-containing amphiphilic block copolymer. Toward this end, a poly(ethylene oxide)-block-poly(sodium *p*-styrenesulfonate) (PEO-*b*-PSSNa) diblock copolymer was synthesized; this diblock copolymer was then incorporated into epoxy to obtain the nanostructured thermosets via a self-assembly approach. The purpose of this work is twofold: (i) to investigate the formation of polyelectrolyte nanophases by the use of a diblock-copolymer-containing polyelectrolyte subchain and (ii) to examine the dielectric properties of epoxy thermosets containing polyelectrolyte nanophases to establish the correlation of the properties with the nanostructures. The PEO-*b*-PSSNa diblock copolymer used in this work was synthesized via the radical polymerization of sodium *p*-styrenesulfonate, which was mediated with 4-cyano-4-(thiobenzoylthio)valeric ester-terminated poly(ethylene oxide). The morphologies of the PSSNa nanophases in the epoxy thermosets were examined by means of transmission electron microscopy (TEM), small-angle X-ray scattering (SAXS), and dynamic mechanical thermal analysis (DMTA). The dielectric properties were measured by means of a broadband dielectric spectroscopy (BDS).

EXPERIMENTAL SECTION

Materials. The epoxy monomer, diglycidyl ether of bisphenol A (DGEBA), was purchased from Shanghai Resin Co., China; it has the epoxide equivalent weight of 185–210. 4,4'-Methylenebis(2-chloroaniline) (MOCA) and 4-dimethylaminopyridine (DMAP) were of chemically pure grade, supplied by Shanghai Reagent Co., China, and were used as received. 4,4'-Azobis(4-cyanopentanoic acid) (ACPA) was purchased from Sigma Co., China; it was recrystallized from ethanol twice before use. 1-(3-(Dimethylamino)propyl)-3-ethylcarbodiimide hydrochloride (EDC) was of analytically pure grade, obtained from Aladdin Co., China. Sodium *p*-styrenesulfonate (SSNa) was purchased from Shanghai Reagent Co., China. Before use, SSNa was purified by recrystallization from the mixture of methanol with water (80/20 vol). Poly(ethylene oxide) monomethyl ether (MPEO5000) was purchased from Sigma Co. Shanghai; it had a quoted molecular weight of $M_n = 5000$ Da. 4-Cyano-4-(thiobenzoylthio) valeric acid (CTBTVA) was synthesized by following the method of the literature.^{57–59} All of the solvents were obtained from commercial resources and were purified according to standard procedures before use.

Synthesis of Macromolecular Chain Transfer Agent. To a flask, poly(ethylene oxide) monomethyl ether (5.010 g, 1.0 mmol), CTBTVA (0.70 g, 2.5 mmol), EDC (0.480 g, 2.5

mmol), DMAP (0.060 g, 0.5 mmol), and dichloromethane (20 mL) were charged with vigorous stirring. The mixture was bubbled with highly pure nitrogen for 1 h. At 25 °C, the esterification reaction was performed for 48 h. The reacted mixture was washed with the saturated aqueous solution of sodium chloride three times (10 mL × 3). The dichloromethane layer was dried with anhydrous MgSO₄ overnight. Thereafter, the solution was dropwise added into diethyl ether to afford the pink precipitates. The precipitates were redissolved with dichloromethane and then redropped into diethyl ether. This procedure was repeated three times. After drying in a vacuum oven at 30 °C for 24 h, the macromolecular chain transfer agent (denoted PEO-CTA) (3.560 g) was obtained with a yield of 71%. ¹H NMR (D₂O, ppm): 7.33–7.90 [*m*, 5H, C₆H₅], 4.09 [*t*, 2H, CH₂CH₂OCOCH₂], 3.53 [*s*, 4H, OCH₂CH₂O], 3.21 [*s*, 3H, CH₃OCCH₂CH₂], 2.58 [*t*, 2H, OCOCH₂CH₂C], 2.45 [*t*, 2H, OCOCH₂CH₂C], 1.79 [*s*, 3H, OCOCH₂CH₂C(CN)CH₃].

Synthesis of PEO-*b*-PSSNa Diblock Copolymer. The above PEO-CTA (2.100 g, 0.42 mmol), SSNa (2.350 g, 11.4 mmol), ACPA (22 mg, 0.08 mmol), and deionized water (8 mL) were added to a flask with vigorous stirring. To remove a trace of oxygen, the flask was connected to a Schlenk line to degas with three freeze–evacuate–thaw cycles. The polymerization was performed at 70 °C for 24 h. The polymerized mixture was dialyzed with deionized water for 3 days to remove the unreacted monomer (viz., SSNa). The aqueous solution of the block copolymer was subjected to rotary evaporation to remove a majority of water. After drying *in vacuo* at 45 °C for 24 h, the diblock copolymer (3.810 g) was obtained and the conversion of the monomer was estimated to be ca. 73%. ¹H NMR (D₂O, ppm): 7.70–6.0 [*m*, 4H, C₆H₄SO₃Na], 4.09 [*t*, 2H, CH₂CH₂OCOCH₂], 3.49 [*t*, 4H, OCH₂CH₂O], 3.16 [*s*, 3H, CH₃OCCH₂CH₂], 2.58 [*t*, 2H, OCOCH₂CH₂C], 2.45 [*t*, 2H, OCOCH₂CH₂C], 1.95–0.86 [*m*, 3H, CH₂CH(C₆H₄SO₃Na)]. GPC: $M_n = 8900$ Da with $M_w/M_n = 1.31$.

Preparation of Nanostructured Epoxy Thermosets.

The PEO-*b*-PSSNa diblock copolymer was dissolved in the mixture of DMF and water (80:20 vol), and then, the solution was added to a desired amount of DGEBA with vigorous stirring. The majority of the solvent was evaporated out at 100 °C with continuous stirring, and the residual solvent was eliminated in a vacuum oven at 100 °C for 24 h. With vigorous stirring, the curing agent (i.e., MOCA) was added until a full dissolution was attained, and then, the mixture was poured into a Teflon mold. All the mixtures were cured at 150 °C for 3 h plus 180 °C for 2 h. The epoxy thermosets were prepared with contents of the PEO-*b*-PSSNa diblock copolymer of 10, 20, 30, and 40 wt %, respectively.

Measurements. *Nuclear Magnetic Resonance (NMR) Spectroscopy.* The ¹H NMR spectroscopy was carried out on a Varian Mercury Plus 400 MHz NMR spectrometer. The samples were dissolved in deuterium chloroform, and the solutions were measured at 25 °C. For the measurements of PEO-CTA and PEO-*b*-PSSNa, deuterium water (D₂O) was used to dissolve the polymers. The chemical shift was read with tetramethylsilane as an external reference.

Size Exclusion Chromatography (SEC). The measurements of molecular weights were conducted on a Waters 717 Plus autosampler apparatus, which was equipped with Waters RH columns and a Dawn Eos (Wyatt Technology) multiangle laser light scattering detector. All the experiments were carried out at

25 °C with water containing NaNO₃ (0.1 M) as the eluent at a rate of 1.0 mL/min.

Transmission Electron Microscopy (TEM). The samples of thermosets were sliced into sections with a thickness of about 70 nm by using an ultrathin microtome machine. The specimens of the sections were stained with RuO₄ for about 10 min and then were placed in 200 mesh copper grids. The morphological observation was conducted on a JEOL JEM 2100F transmission electron microscope at a voltage of 120 kV.

Small-Angle X-ray Scattering (SAXS). All the SAXS experiments were performed on the small-angle X-ray scattering station (BL16B1) in the Shanghai Synchrotron Radiation Facility, China, in which the third generation of synchrotron radiation light source had an X-ray wavelength of $\lambda = 1.24 \text{ \AA}$. For the measurements at elevated temperatures, a TH MS600 Linkam hot stage with a precision of 0.1 °C was used as an insertion device. Two-dimensional diffraction patterns were recorded by using an image intensified CCD detector. The intensity profiles were output as the plots of scattering intensity (I) as functions of scattering vector, $q = (4\pi/\lambda) \sin(\theta/2)$ (θ = scattering angle).

Dynamic Mechanical Thermal Analysis (DMTA). The DMTA measurements were conducted on a TA Instruments DMA Q800 dynamic mechanical thermal analyzer (DMTA) in a single cantilever mode. The rectangle specimens with the dimension of $1.2 \times 2 \times 0.1 \text{ cm}^3$ were measured with the frequency of 1.0 Hz and at a heating rate of 3.0 °C/min. The measurements were performed from -80 to 200 °C.

Dielectric Measurements. The control epoxy (and/or nanostructured epoxy) thermoset was machined into a cylinder with a height of ca. 50 mm and a diameter of 200 mm. The surfaces were highly polished. Before the measurements, two aluminum foils were pasted on the surfaces of the cylinder and used as the working electrodes. Permittivity and dielectric loss were measured on an impedance analyzer (Agilent 4294A) with a 16451B dielectric test fixture in the frequency range 10^3 – 10^7 Hz, applying 0.5 V of alternating current voltage across two sides of the disk-shaped specimens.

RESULTS AND DISCUSSION

Synthesis of PEO-*b*-PSSNa Diblock Copolymer. The route of synthesis for the PEO-*b*-PSSNa diblock copolymer is shown in Scheme 1. A reversible addition–fragmentation chain transfer (RAFT) polymerization approach was used to synthesize the diblock copolymer. First, the macromolecular chain transfer agent was prepared via the etherification reaction of poly(ethylene oxide) monomethyl ether with 4-cyanopentanoic acid dithiobenzoate (CTBTVA). Second, the radical polymerization of sodium *p*-styrenesulfonate (SSNa) was carried out and mediated with the above 4-cyano-4-(thiobenzoylthio)valeric ester-terminated poly(ethylene oxide) (denoted PEO-CTA) to afford the PEO-*b*-PSSNa diblock copolymer. The ¹H NMR spectra of CTBTVA, PEO-CTA, and the PEO-*b*-PSSNa diblock copolymer are shown in Figure 1. For CTBTVA, the peaks of resonance at 1.9 and 2.3–2.9 ppm are assignable to the protons of methyl and methylene groups; those at 7.33–7.90 ppm, to the protons of the monosubstituted phenyl groups. For PEO-CTA, there appeared an intense peak centered at 3.53 ppm besides all the peaks assignable to the protons of CTBTVA. This peak is attributable to the protons of methylene groups in the backbone of PEO. In addition, the single peak at 3.21 ppm is assignable to the resonance of the terminal methyl protons of the PEO. Notably, the resonance of

Scheme 1. Synthesis of PEO-CTA and PSSNa-*b*-PEO Diblock Copolymer

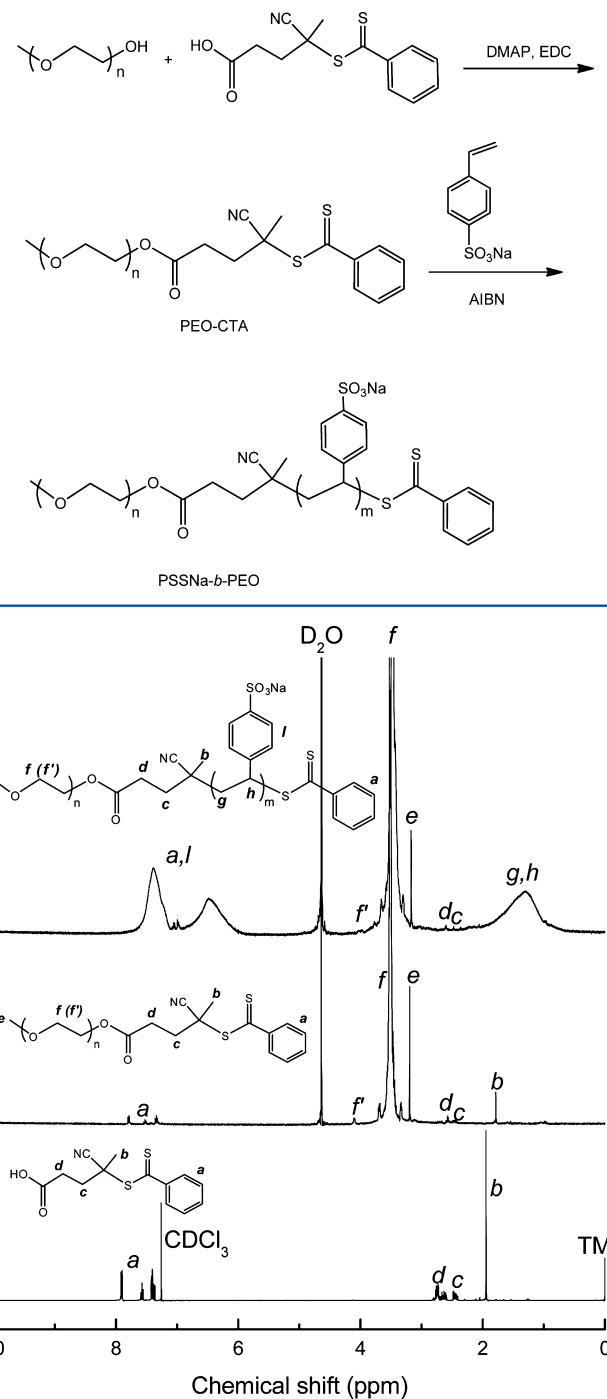


Figure 1. ¹H NMR spectra of 4-cyanopentanoic acid dithiobenzoate, PEO-CTA, and PSSNa-*b*-PEO diblock copolymer.

methyl protons in CTBTVA upfield shifted to 1.78 ppm with the occurrence of the esterification. In terms of the ratio of the integral intensity of the resonance at 3.21 ppm to that at 3.53 ppm, the length of the PEO chain was calculated to be $M_n = 5100 \text{ Da}$ and this value was quite close to the quoted molecular weight provided by the manufacturer. For the PEO-*b*-PSSNa diblock copolymer, the signal of resonance at 7.70–6.01 ppm was characteristic of phenyl protons of PSSNa block; the broad peaks at 1.95–0.86 ppm were attributable to the protons of

methylene and methine in the main chains of PSSNa. Notably, all the signals assignable to PEO chains were discernible as in PEO-CTA. The ^1H NMR spectroscopy indicates that the resulting polymer combined the structural features from both PEO and PSSNa blocks. The diblock copolymer was subjected to size exclusion chromatography (SEC) to measure its molecular weight, and the SEC curve is shown in Figure 2. A

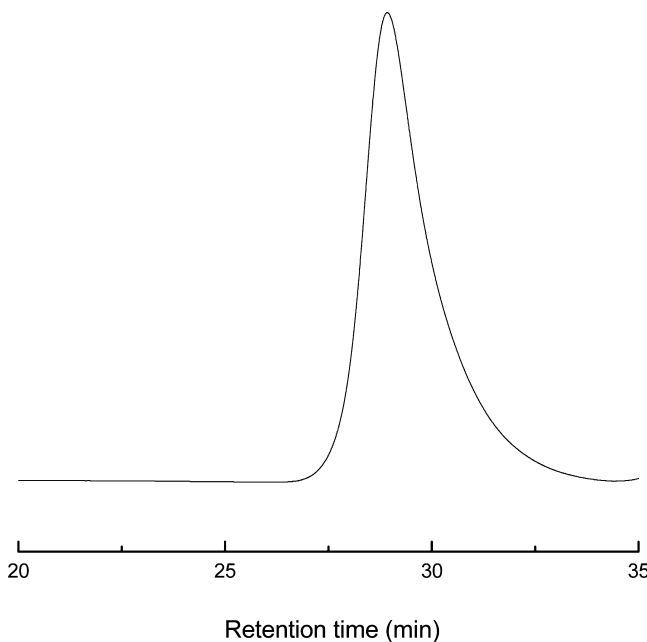


Figure 2. SEC curve of the PSSNa-*b*-PEO diblock copolymer.

unimodal distribution of molecular weight was exhibited, and the molecular weight was measured to be $M_n = 8900$ Da with $M_w/M_n = 1.31$. The SEC result indicates that the RAFT polymerization was successfully carried out; i.e., the PEO-*b*-PSSNa diblock copolymer was successfully obtained.

Formation of PSSNa Nanophases in Epoxy Thermosets. The above PEO-*b*-PSSNa diblock copolymer was incorporated into epoxy to prepare the thermosetting blends. At room and elevated temperatures, all the mixtures composed of diblock copolymer and the precursors of epoxy (i.e., DGEBA and MOCA) were homogeneous and transparent, suggesting that no macroscopic phase separation occurred. The thermosetting blends were obtained by curing at 150 °C for 3 h plus 180 °C for 2 h. Notably, all the cured blends were still homogeneous and transparent, implying that no macroscopic phase separation occurred in the process of the curing reaction. Nonetheless, the clarity did not exclude the possible microphase separation in the thermosetting blends because PSSNa was inherently immiscible with epoxy. In this work, the morphologies of the thermosetting blends were investigated by means of transmission electronic microscopy (TEM), small-angle X-ray scattering (SAXS), and dynamic mechanical thermal analysis (DMTA).

Before the morphological observation with TEM, the sections of all the samples were stained with RuO₄. In views of the chemical structures of the components in the thermosetting blends, it is proposed that the epoxy matrix would be stained with RuO₄, whereas PSSNa blocks remained invariant. Shown in Figure 3 are the TEM micrographs of the blends containing 10, 20, 30, and 40 wt % PEO-*b*-PSSNa.

Notably, all these samples displayed the microphase-separated morphologies, in which the spherical microdomains with a size of 35–45 nm in diameter were dispersed into the continuous matrix (see Figure 3A–C). The number of spherical microdomains increased with increasing content of PEO-*b*-PSSNa diblock copolymer. While the concentration of PEO-*b*-PSSNa diblock copolymer was 40 wt %, some cylindrical microdomains appeared (see Figure 3D). According to the volume fraction of the diblock copolymer and the miscibility of all the component polymers, the light and spherical microdomains are assignable to the PSSNa block, whereas the dark and continuous matrix is assignable to epoxy which could be miscible with the PEO block. The TEM results showed that PSSNa nanophases were indeed formed in the thermosets. All the cured blends were subjected to SAXS, and the SAXS profiles are presented in Figure 4. It is seen that the scattering profiles were exhibited for all the thermosetting blends containing PEO-*b*-PSSNa diblock copolymer. The SAXS results indicate that the thermosetting blends of epoxy with PEO-*b*-PSSNa diblock copolymer were indeed microphase-separated; i.e., the PSSNa nanophases were formed in the thermosetting epoxy matrixes.

It has been realized that the formation of nanophases can follow the self-assembly^{22,23} or reaction-induced microphase separation (RIMPS)^{24,25} mechanism depending on the miscibility of copolymer subchains with thermosets before and after curing reaction. In the present case, the diblock copolymer used to control the formation of nanophases contained a polyelectrolyte subchain (viz., PSSNa). To judge the formation mechanism of the nanophases, the microphase separation behavior of the thermosetting system after and before the curing reaction was examined. Toward this end, variable temperature SAXS experiments were carried out. Representatively shown in Figure 5 are the SAXS profiles of the mixture of epoxy with 40 wt % PEO-*b*-PSSNa diblock copolymer at 25 and 150 °C and the mixture cured at 150 °C for 3 h. At 25 °C, one scattering peak at ca. 0.29 nm⁻¹ was discernible, indicating that the mixture was microphase-separated. The microphase-separated morphology is accounted for by the self-assembly behavior of PEO-*b*-PSSNa diblock copolymer in the precursors of epoxy. In other words, the epoxy precursors could act as the selective solvent of the diblock copolymer and the self-assembled nanophases were formed. While this mixture was heated up to 150 °C (viz., the curing temperature), notably, the scattering peak did not disappear but shifted to $q = 0.20 \text{ nm}^{-1}$. This observation indicates that the self-assembled nanophases still existed at the beginning of the curing reaction; i.e., the curing reaction would occur in the presence of self-assembled nanophases. The shift of the scattering peak to the position at a lower q value indicates that the average distance between adjacent PSSNa microdomains increased. The increased average intermicrodomain distance at 150 °C could result from the demixing of the epoxy precursors out of the PSSNa-rich nanophases. After the mixture was cured at 150 °C for 3 h, the shape of the scattering curve remained almost unchanged but the intensity of the scattering peaks increased. The results of SAXS indicate that the formation of the PSSNa nanophase in the epoxy thermosets containing a PEO-*b*-PSSNa diblock copolymer followed the self-assembly mechanism.

The formation of PSSNa nanophases is attributable to the difference in miscibility of both of the copolymer subchains (viz., PEO and PSSNa) with the epoxy thermoset, which was

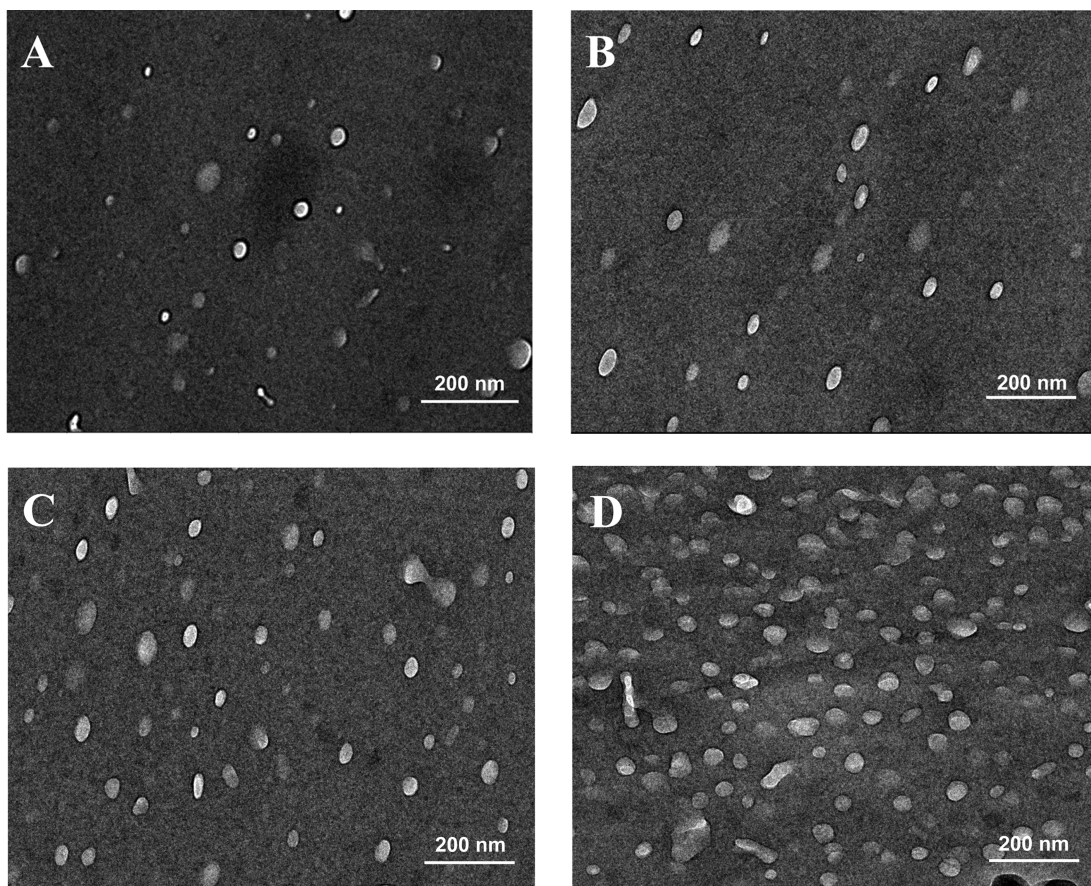


Figure 3. TEM images of the epoxy thermosets containing 10 (A), 20 (B), 30 (C), and 40 wt % (D) PSSNa-*b*-PEO diblock copolymer.

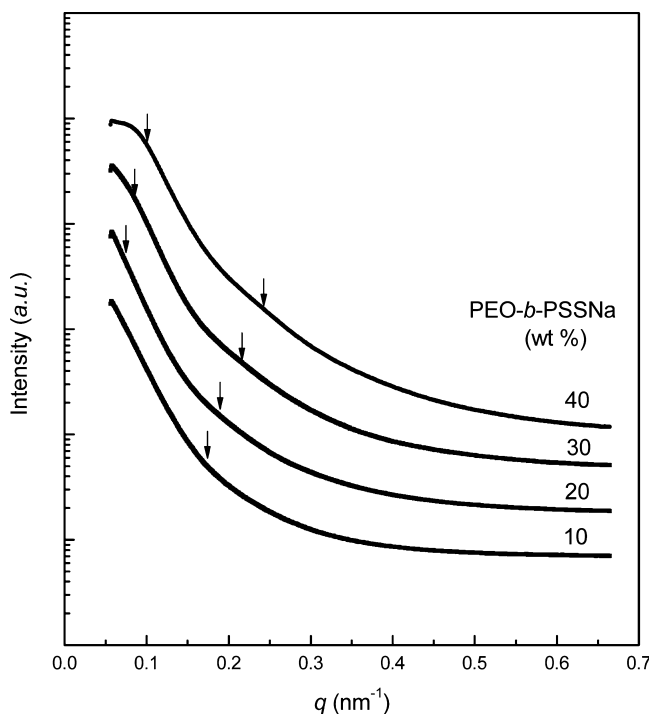


Figure 4. SAXS profiles of the epoxy thermosets containing PEO-*b*-PSSNa diblock copolymers.

readily investigated with dynamic mechanical thermal analysis (DMTA). The DMTA spectra are shown in Figure 6. The

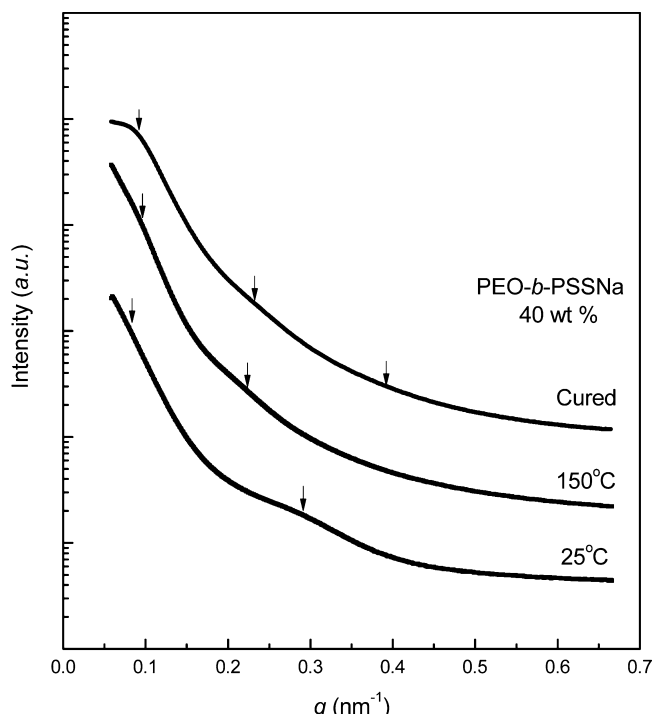


Figure 5. SAXS profiles of the mixture containing 40 wt % PSSNa-*b*-PEO diblock copolymers: at 25 °C, at 150 °C, and after being cured at 150 °C for 3 h plus 180 °C for 2 h.

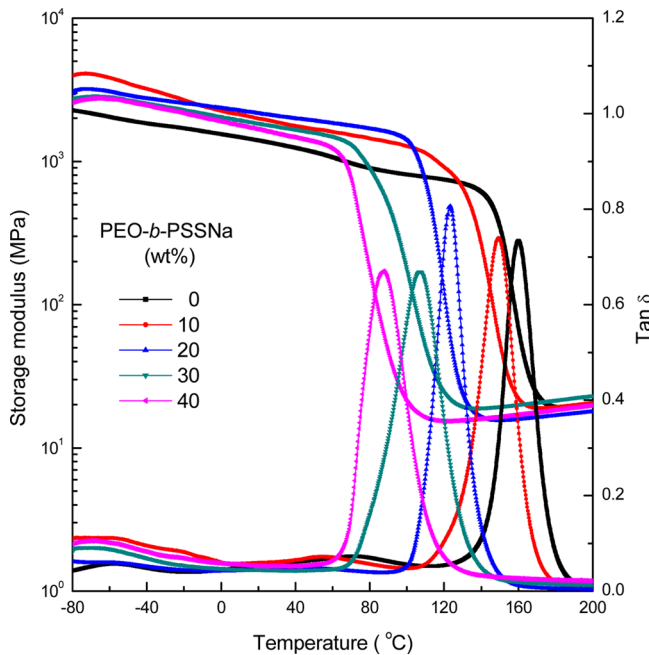
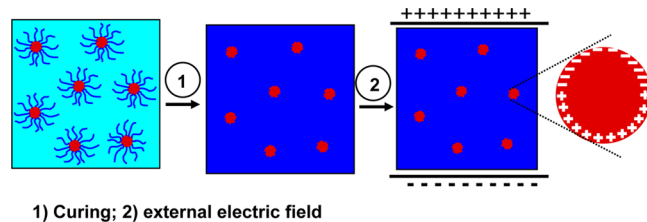


Figure 6. DMTA curves of the epoxy thermosets containing PSSNa-*b*-PEO diblock copolymer.

control epoxy displayed a well-defined α transition at ca. 159 °C; this peak is associated with the glass–rubber transition of the thermosetting polymer. Besides the α transition, two secondary transitions (viz., β -relaxations) were exhibited at \sim –56 and 73 °C, respectively. The former is responsible for the motion of hydroxyl ether structural units of aromatic amine-cross-linked epoxy, whereas the latter to that of diphenyl groups in epoxy.^{60–62} Upon adding PEO-*b*-PSSNa diblock copolymer into the thermoset, notably, the α transitions shifted to the low temperatures and the temperatures of the transition decreased with increasing content of PEO-*b*-PSSNa. The depressed temperatures of α peaks (i.e., T_g 's) are ascribed to the plasticization of PEO blocks on the epoxy matrixes.^{63,64} The miscibility of PEO chains with the epoxy was further evidenced by the fact that the β transitions at –56 and 73 °C became indiscernible in the nanostructured thermosets. This phenomenon can be explained by the antiplasticization of PEO on the epoxy networks. The intimate mixing of PEO chains with epoxy networks could suppress the motion of the secondary transition structural units.^{60–62} It should be pointed out that the glass transition temperature of PSSNa micro-domains could be too high to be detected in the present range of temperature. The high T_g of PSSNa nanophases could result from the very strong ionic bonding interactions in the polyelectrolyte. In addition, it is noted that, in the glassy state, all the epoxy nanocomposites containing PEO-*b*-PSSNa displayed a storage modulus much higher than the control epoxy. The enhanced moduli for the nanostructured thermosets could be ascribed to the nanoreinforcement of the PSSNa nanophases on the epoxy matrixes.

Dielectric Properties of Epoxy Thermosets Containing PSSNa Nanophases. The results of SAXS, TEM, and DMTA showed that the PSSNa nanophases were formed in the epoxy thermosets (see Scheme 2). Compared to the control epoxy, two additional components (i.e., PEO and PSSNa) were introduced into the thermosets. Of them, PEO remained intimately mixed with the epoxy network, whereas PSSNa was

Scheme 2. Formation of PSSNa Nanophases in Epoxy Thermosets and the Polarization of the Nanocomposites under an External Electric Field



demixed out of the epoxy in the form of nanodomains. To isolate the effect of the PSSNa nanophases on the dielectric properties of the nanostructured thermosets, it is mandatory to know the effect of the segmental inclusion of PEO into the epoxy matrixes. For this purpose, we prepared the binary thermosetting blends of epoxy with PEO by controlling the contents of PEO to be identical with those in the nanostructured thermosets. The binary thermosetting blends were subjected to the dielectric measurements. Shown in Figures 7

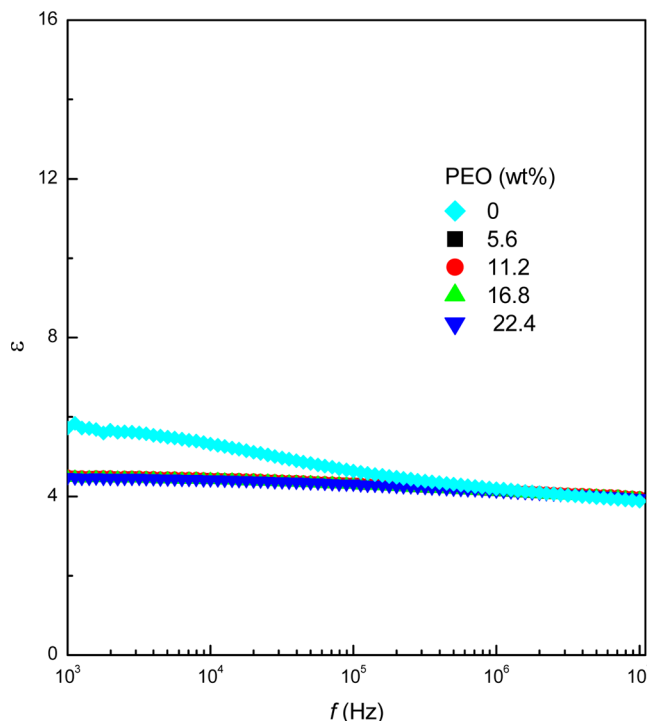


Figure 7. Plots of dielectric constants of the control epoxy and the binary thermosetting blends of epoxy and PEO as functions of AC frequency.

and 8 are the plots of dielectric constant (ϵ) and dielectric loss ($\tan \delta$) as functions of AC frequency at 25 °C, respectively. With inclusion of the miscible PEO, notably, both dielectric constants and dielectric loss were slightly decreased, especially at the lower AC frequencies. The decreased ϵ and $\tan \delta$ values could be explained on the basis of the inclusion of the diluent (viz., PEO). In other words, the concentrations of the dipoles in the binary blends were lower than that in the control epoxy, since PEO could act as the inert diluent of the dipoles. In addition, the inclusion of PEO with the concentrations investigated (viz., 5.6, 11.2, 16.8, and 22.4 wt %) would not significantly change the mobility of the dipoles in the

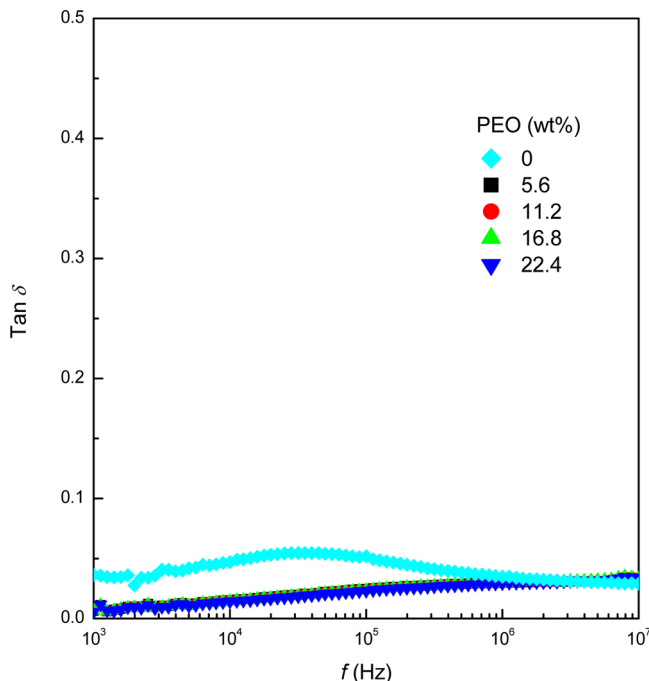


Figure 8. Plots of dielectric loss tangent of the control epoxy and the binary thermosetting blends of epoxy and PEO at 25 °C as functions of AC frequency.

thermosets at the present experimental temperature (i.e., 25 °C).

All the nanostructured epoxy thermosets containing PSSNa nanophases were subjected to the dielectric measurements. The plots of dielectric constant (ϵ) and dielectric loss ($\tan \delta$) as functions of AC frequency at 25 °C were presented in Figures 9 and 10, respectively. The dielectric constant of the plain epoxy

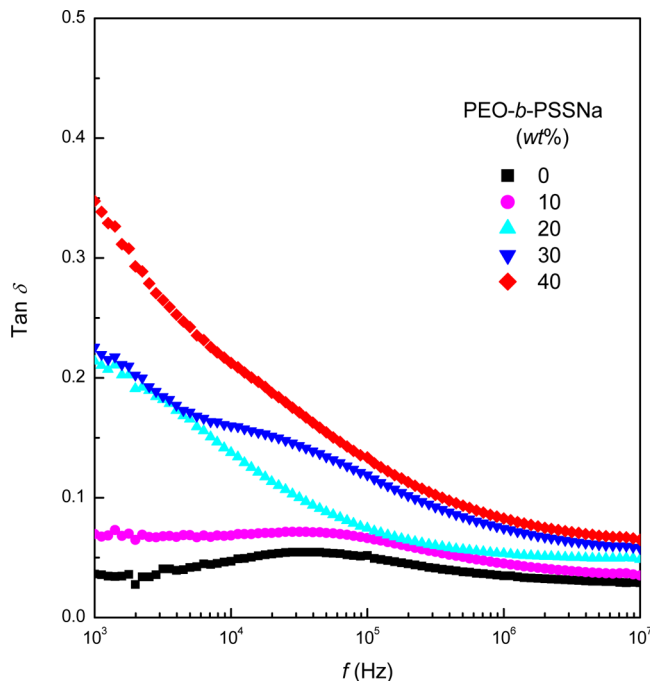


Figure 10. Plots of the dielectric loss tangent of the control epoxy and the nanostructured thermosets containing PSSNa-*b*-PEO diblock copolymer at 25 °C as functions of AC frequency.

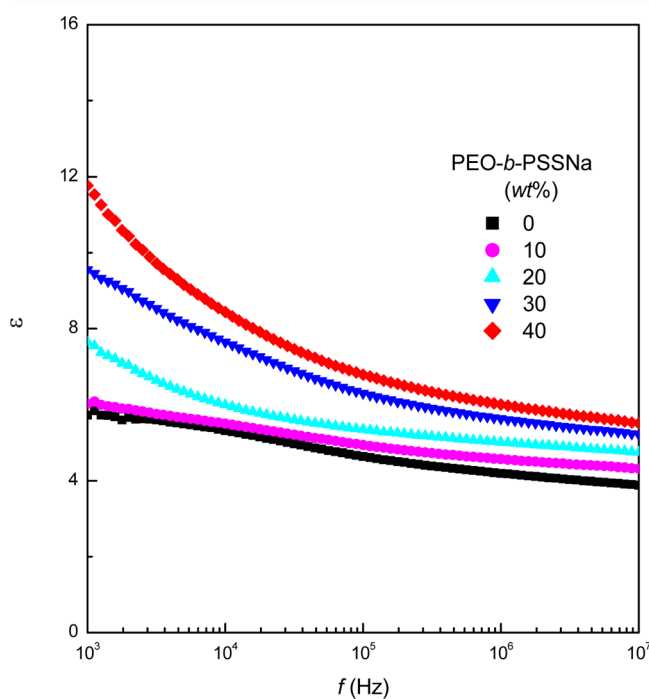


Figure 9. Plots of dielectric constants of the control epoxy and the nanostructured thermosets containing PSSNa-*b*-PEO diblock copolymer at 25 °C as functions of AC frequency.

was measured to be $\epsilon = 5.84$ at a frequency of 10³ Hz. After PEO-*b*-PSSNa was added to the epoxy, the dielectric constants of the nanostructured thermosets were significantly enhanced; the dielectric constants were enhanced with increasing concentration of PEO-*b*-PSSNa. For the nanostructured thermoset containing 40 wt % PEO-*b*-PSSNa, the dielectric constant was increased up to $\epsilon = 11.9$ at a frequency of 10³ Hz; the ϵ value increased about 200%. The increased dielectric constants were attributable to the formation of PSSNa nanophases in the thermosets. It is proposed that the interface polarization in the nanostructured thermosets could be significantly promoted, since a great amount of the interface between PSSNa microdomains and epoxy matrixes was created owing to the formation of PSSNa nanophases. According to the Maxwell-Wagner polarization mechanism,^{65,66} there was an additional charge accumulation at the interface between PSSNa nanophases and the epoxy matrix under an external electrical field (see Scheme 2). While the frequencies of the applied alternating field were sufficiently low, the charges near PSSNa-epoxy interfaces began to build up (conductivity effect) and opposed the external electrical field. As a consequence, the effective field acting on the PSSNa microdomains reduced its strength. At sufficiently high frequencies of an applied electric field, the depolarization field effects in the nanostructured thermosets vanished, since the movement of charges failed to come up with the high frequencies and the development of depolarization fields was interrupted. The dielectric constants of the PSSNa-containing thermosets decreased with increasing AC frequency as the control epoxy. Nonetheless, the dielectric constants of the nanostructured thermosets decreased much faster than the control epoxy with increasing AC frequency. This observation suggests that with increasing AC frequency the polarization of the PSSNa microdomains failed to keep up with the electric field. For control epoxy, the dielectric loss ($\tan \delta$) remained almost invariant regardless of the AC frequency

(see Figure 10), suggesting that the mobility of the dipoles in the cross-linked network was not sufficiently strong to cause the dissipation of energy with increasing frequency of applied electric field. After adding PEO-*b*-PSSNa diblock copolymer to the control epoxy, the dielectric loss was increased at the low frequency (viz., 10³ Hz) of electric field, as shown in Figure 10. The increased dielectric loss is attributable to the incorporation of the charge carriers (viz., PSSNa microdomains) with relatively high mobility. In addition, the increased dielectric loss was also related to the interfacial polarization relaxation in PSSNa nanophases in the nanostructured thermosets. With increasing frequency of the applied electric field, however, the movement of the charge carrier and the interfacial polarization relaxation increasingly failed to keep up with the electric field in the nanocomposites. As a consequence, the values of dielectric loss were decreased with increasing electric field frequency. Compared to control epoxy, nonetheless, the dielectric loss of the nanostructured thermosets still remained at quite a low level, although the values of dielectric loss were slightly increased with inclusion of PSSNa nanophases.

CONCLUSIONS

Poly(ethylene oxide)-block-poly(sodium *p*-styrenesulfonate) was successfully synthesized via the reversible addition-fragmentation chain transfer polymerization (RAFT) approach. This diblock copolymer was introduced into epoxy thermosets, and the PSSNa nanophases were formed via the self-assembly approach. The formation of PSSNa nanophases in the epoxy thermoset was evidenced by means of small-angle X-ray scattering (SAXS), transmission electron microscopy (TEM), and dynamic mechanical thermal analysis (DMTA). The PSSNa nanophases exerted the nanoreinforcement on the matrixes of the nanocomposites in the glassy state. With the incorporation of PSSNa nanophases, more importantly, the dielectric constants of the thermosets were significantly enhanced. In the meantime, the dielectric loss values were slightly increased with inclusion of PSSNa nanophases.

AUTHOR INFORMATION

Corresponding Author

*E-mail: szheng@sjtu.edu.cn. Phone: 86-21-54743278. Fax: 86-21-54741297.

Notes

The authors declare no competing financial interest.

ACKNOWLEDGMENTS

The financial support from Natural Science Foundation of China (Nos. 51133003 and 21274091) was gratefully acknowledged. The authors thank the Shanghai Synchrotron Radiation Facility for the support under Project Nos. 10sr0260 and 10sr0126.

REFERENCES

- Pascault, J. P.; Williams, R. J. J. Formulation and Characterization of Thermoset/Thermoplastic Blends. *Polymer Blends*; Wiley: New York, 2010; Vol. 1, pp 379–415.
- Zheng, S. Nanostructured Epoxies by the Use of Block Copolymers. *Epoxy Polymers: New Materials and Innovations*; Wiley-VCH: Weinheim, Germany, 2010; pp 79–108.
- Guo, Q. Thermosets: Structure, Properties and Applications. *Polymer Blends and Alloys*; Marcel Dekker: New York, 1999; Chapter 6, pp 155–187.

(4) Ulrich, R. K.; Schaper, L. W. *Integrated Passive Component Technology*; IEEE Press, Wiley-Interscience: Hoboken, NJ, 2003.

(5) Prymark, J.; Bhattacharya, S.; Paik, K.; Tummala, R. R. *Fundamentals of Microsystems Packaging*; McGraw-Hill: New York, 2001.

(6) Sharma, R. A.; D'Melo, D.; Bhattacharya, S.; Chaudhari, L.; Swain, S. Effect of Nano/micro Silica on Electrical Property of Unsaturated Polyester Resin Composites. *IEEE Trans. Dielectr. Electr. Insul.* **2012**, *13*, 31–34.

(7) Wang, Z.; Nelson, J. K.; Hillborg, H.; Zhao, S.; Schadler, L. S. Graphene Oxide Filled Nanocomposite with Novel Electrical and Dielectric Properties. *Adv. Mater.* **2012**, *24*, 3134–3137.

(8) Yu, A. P.; Ramesh, P.; Itkis, M. E.; Belyarova, E.; Haddon, R. C. Graphite Nanoplatelet-Epoxy Composite Thermal Interface Materials. *J. Phys. Chem. C* **2007**, *111*, 7565–7569.

(9) Li, Y.; Pothukuchi, S.; Wong, C. P. *Proceedings of the 54th Ieee Electronic Components and Technology Conference*; Las Vegas, NV, 2004; pp 507–513.

(10) Psarras, G. C.; Manolakaki, E.; Tsangaris, G. M. Electrical Relaxations in Polymeric Particulate Composites of Epoxy Resin and Metal Particles. *Composites, Part A* **2002**, *33*, 375–384.

(11) Bai, Y.; Cheng, Z. Y.; Bharti, V.; Xu, H. S.; Zhang, Q. M. High-Dielectric-Constant Ceramic-Powder Polymer Composites. *Appl. Phys. Lett.* **2000**, *76*, 3804–3806.

(12) Shen, Y.; Gu, A.; Liang, G.; Yuan, L. High Performance CaCu₃Ti₄O₁₂/Cyanate Ester Composites With Excellent Dielectric Properties and Thermal Resistance. *Composites, Part A* **2010**, *41*, 1668–1676.

(13) Wang, L.; Dang, Z.-M. Carbon Nanotube Composites with High Dielectric Constant at Low Percolation Threshold. *Appl. Phys. Lett.* **2005**, *87*, 042903–042906.

(14) Dang, Z. M.; Wang, L.; Yin, Y.; Zhang, Q.; Lei, Q. Q. Giant Dielectric Permittivities in Functionalized Carbon-Nanotube/Electroactive-Polymer Nanocomposites. *Adv. Mater.* **2007**, *19*, 852–857.

(15) Yang, C.; Lin, Y. H.; Nan, C. W. Modified Carbon Nanotube Composites with High Dielectric Constant, Low Dielectric Loss and Large Energy Density. *Carbon* **2009**, *47*, 1096–1101.

(16) Zhang, J.; Mine, M.; Zhu, D.; Matsuo, M. Electrical and Dielectric Behaviors and Their Origins in the Three-Dimensional Polyvinyl Alcohol/Mwcnt Composites with Low Percolation Threshold. *Carbon* **2009**, *47*, 1311–1320.

(17) Jiang, M. J.; Dang, Z. M.; Bozlar, M.; Miomandre, F.; Bai, J. Broad-frequency Dielectric Behaviors in Multiwalled Carbon Nanotube/Rubber Nanocomposites. *J. Appl. Phys.* **2009**, *50*, 106–112.

(18) Lu, J.; Moon, K. S.; Kim, B. K.; Wong, C. P. High Dielectric Constant Polyaniline/Epoxy Composites via in Situ Polymerization for Embedded Capacitor Applications. *Polymer* **2007**, *48*, 1510–1516.

(19) Wang, J. W.; Wang, Y.; Wang, F.; Li, S. Q.; Xiao, J.; Shen, Q. D. A Large Enhancement in Dielectric Properties of Poly(vinylidene fluoride) Based All-organic Nanocomposite. *Polymer* **2009**, *50*, 679–684.

(20) Dang, Z. M.; Wang, L.; Yin, Y.; Zhang, Q.; Lei, Q. Q. Giant Dielectric Permittivities in Functionalized Carbon-nanotube/Electroactive-polymer Nanocomposites. *Adv. Mater.* **2007**, *19*, 852–857.

(21) Wang, C. C.; Song, J. F.; Bao, H. M.; Shen, Q. D.; Yang, C. Z. Enhancement of Electrical Properties of Ferroelectric Polymers by Polyaniline Nanofibers with Controllable Conductivities. *Adv. Funct. Mater.* **2008**, *18*, 1299–1306.

(22) Hillmyer, M. A.; Lipic, P. M.; Hajduk, D. A.; Almdal, K.; Bates, F. S. Self-Assembly and Polymerization of Epoxy Resin-Amphiphilic Block Copolymer Nanocomposites. *J. Am. Chem. Soc.* **1997**, *119*, 2749–2750.

(23) Lipic, P. M.; Bates, F. S.; Hillmyer, M. A. Nanostructured Thermosets from Self-Assembled Amphiphilic Block Copolymer/Epoxy Resin Mixtures. *J. Am. Chem. Soc.* **1998**, *120*, 8963–8970.

(24) Meng, F.; Zheng, S.; Zhang, W.; Li, H.; Liang, Q. Nanostructured Thermosetting Blends of Epoxy Resin and Amphiphilic Poly(*ε*-caprolactone)-block-polybutadiene-block-poly(*ε*-caprolactone) Triblock Copolymer. *Macromolecules* **2006**, *39*, 711–719.

- (25) Meng, F.; Zheng, S.; Li, H.; Liang, Q.; Liu, T. Formation of Ordered Nanostructures in Epoxy Thermosets: A Mechanism of Reaction-Induced Microphase Separation. *Macromolecules* **2006**, *39*, 5072–5080.
- (26) Mijovic, J.; Shen, M.; Sy, J. W.; Mondragon, I. Dynamics and Morphology in Nanostructured Thermoset Network/Block Copolymer Blends During Network Formation. *Macromolecules* **2000**, *33*, 5235–5244.
- (27) Grubbs, R. B.; Dean, J. M.; Broz, M. E.; Bates, F. S. Reactive Block Copolymers for Modification of Thermosetting Epoxy. *Macromolecules* **2000**, *33*, 9522–9534.
- (28) Grubbs, R. B.; Dean, J. M.; Bates, F. S. Methacrylic Block Copolymers through Metal-Mediated Living Free Radical Polymerization for Modification of Thermosetting Epoxy. *Macromolecules* **2001**, *34*, 8593–8595.
- (29) Guo, Q.; Thomann, R.; Gronski, W.; Thurn-Albrecht, T. Phase Behavior, Crystallization, and Hierarchical Nanostructures in Self-Organized Thermoset Blends of Epoxy Resin and Amphiphilic Poly(ethylene oxide)-block-poly(propylene oxide)-block-poly(ethylene oxide) Triblock Copolymers. *Macromolecules* **2002**, *35*, 3133–3144.
- (30) Ritzenthaler, S.; Court, F.; David, L.; Girard-Reydet, E.; Leibler, L.; Pascault, J. P. ABC Triblock Copolymers/epoxy-diamine Blends. 1. Keys to Achieve Nanostructured Thermosets. *Macromolecules* **2002**, *35*, 6245–6254.
- (31) Ritzenthaler, S.; Court, F.; Girard-Reydet, E.; Leibler, L.; Pascault, J. P. ABC Triblock Copolymers/epoxy-diamine Blends. 2. Parameters Controlling the Morphologies and Properties. *Macromolecules* **2003**, *36*, 118–126.
- (32) Rebizant, V.; Abetz, V.; Tournilhac, F.; Court, F.; Leibler, L. Reactive Tetrablock Copolymers Containing Glycidyl Methacrylate. Synthesis and Morphology Control in Epoxy-Amine Networks. *Macromolecules* **2003**, *36*, 9889–9896.
- (33) Rebizant, V.; Venet, A. S.; Tournilhac, F.; Girard-Reydet, E.; Navarro, C.; Pascault, J. P.; Leibler, L. Chemistry and Mechanical Properties of Epoxy-Based Thermosets Reinforced by Reactive and Nonreactive SBMx Block Copolymers. *Macromolecules* **2004**, *37*, 8017–8027.
- (34) Dean, J. M.; Verghese, N. E.; Pham, H. Q.; Bates, F. S. Nanostructure Toughened Epoxy Resins. *Macromolecules* **2003**, *36*, 9267–9270.
- (35) Zucchi, I. A.; Galante, M. J.; Williams, R. J. J. Comparison of Morphologies and Mechanical Properties of Crosslinked Epoxies Modified by Polystyrene and Poly(methyl methacrylate)) or by the Corresponding Block Copolymer Polystyrene-*b*-poly(methyl methacrylate). *Polymer* **2005**, *46*, 2603–2609.
- (36) Thio, Y. S.; Wu, J.; Bates, F. S. Epoxy Toughening Using Low Molecular Weight Poly(hexylene oxide)-poly(ethylene oxide) Diblock Copolymers. *Macromolecules* **2006**, *39*, 7187–7189.
- (37) Serrano, E.; Tercjak, A.; Kortaberria, G.; Pomposo, J. A.; Mecerreyres, D.; Zafeiropoulos, N. E.; Stamm, M.; Mondragon, I. Nanostructured Thermosetting Systems by Modification with Epoxidized Styrene-butadiene Star Block Copolymers. Effect of Epoxidation Degree. *Macromolecules* **2006**, *39*, 2254–2261.
- (38) Ocando, C.; Serrano, E.; Tercjak, A.; Peña, C.; Kortaberria, G.; Calberg, C.; Grignard, B.; Jerome, R.; Carrasco, P. M.; Mecerreyres, D.; Mondragon, I. Structure and Properties of a Semifluorinated Diblock Copolymer Modified Epoxy Blend. *Macromolecules* **2007**, *40*, 4068–4074.
- (39) Maiez-Tribut, S.; Pascault, J. P.; Soulé, E. R.; Borrajo, J.; Williams, R. J. J. Nanostructured Epoxies Based on the Self-assembly of Block Copolymers: A New Miscible Block that can be Tailored to Different Epoxy Formulations. *Macromolecules* **2007**, *40*, 1268–1273.
- (40) Sinturel, C.; Vayer, M.; Erre, R.; Amenitsch, H. Nanostructured Polymers Obtained from Polyethylene-*b*-poly(ethylene oxide) Block Copolymer in Unsaturated Polyester. *Macromolecules* **2007**, *40*, 2532–2538.
- (41) Xu, Z.; Zheng, S. Reaction-Induced Microphase Separation in Epoxy Thermosets Containing Poly(ϵ -caprolactone)-block-poly(*n*-butyl acrylate) Diblock Copolymer. *Macromolecules* **2007**, *40*, 2548–2558.
- (42) Meng, F.; Xu, Z.; Zheng, S. Microphase Separation in Thermosetting Blends of Epoxy Resin and Poly(ϵ -caprolactone)-block-polystyrene Block Copolymers. *Macromolecules* **2008**, *41*, 1411–1420.
- (43) Fan, W.; Wang, L.; Zheng, S. Nanostructures in Thermosetting Blends of Epoxy Resin with Polydimethylsiloxane-*b*-block-Poly(ϵ -caprolactone)-block-polystyrene ABC Triblock Copolymer. *Macromolecules* **2009**, *42*, 327–336.
- (44) Ocando, C.; Tercjak, A.; Martín, M. D.; Ramos, J. A.; Campo, M.; Mondragon, I. Morphology Development in Thermosetting Mixtures through the Variation on Chemical Functionalization Degree of Poly(styrene-*b*-butadiene) Diblock Copolymer Modifiers. Thermomechanical Properties. *Macromolecules* **2009**, *42*, 6215–6224.
- (45) Fan, W.; Wang, L.; Zheng, S. Double Reaction-Induced Microphase Separation in Epoxy Resin Containing Polystyrene-*b*-block-poly(ϵ -caprolactone)-block-poly(*n*-butyl acrylate) ABC Triblock Copolymer. *Macromolecules* **2010**, *43*, 10600–10611.
- (46) Serrano, E.; Martín, M. D.; Tercjak, A.; Pomposo, J. A.; Mecerreyres, D.; Mondragon, I. Nanostructured Thermosetting Systems from Epoxidized Styrene Butadiene Block Copolymers. *Macromol. Rapid Commun.* **2005**, *26*, 982–985.
- (47) Hameed, N.; Guo, Q.; Xu, Z.; Hanley, T. L.; Mai, Y. W. Reactive Block Copolymer Modified Thermosets: Highly Ordered Nanostructures and Improved Properties. *Soft Matter* **2010**, *6*, 6119–6129.
- (48) Wu, S.; Guo, Q.; Peng, S.; Hameed, N.; Kraska, M.; Stühn, B.; Mai, Y. W. Toughening Epoxy Thermosets with Block Ionomer Complexes: A Nanostructure-Mechanical Property Correlation. *Macromolecules* **2012**, *45*, 3829–3840.
- (49) Yu, R.; Zheng, S. Morphological Transition from Spherical to Lamellar Nanophases in Epoxy Thermosets Containing Poly(ethylene oxide)-block-poly(ϵ -caprolactone)-block-polystyrene Triblock Copolymer by Hardeners. *Macromolecules* **2011**, *44*, 8546–8557.
- (50) Yu, R.; Zheng, S.; Li, X.; Wang, J. Reaction-Induced Microphase Separation in Epoxy Thermosets Containing Block Copolymers Composed of Polystyrene and Poly(ϵ -caprolactone): Influence of Copolymer Architectures on Formation of Nanophases. *Macromolecules* **2012**, *45*, 9155–9168.
- (51) Garate, H.; Mondragon, I.; D'Accorso, N. B.; Goyanes, S. Exploring Microphase Separation Behavior of Epoxidized Poly(styrene-*b*-isoprene-*b*-styrene) Block Copolymer inside Thin Epoxy Coatings. *Macromolecules* **2013**, *46*, 2182–2187.
- (52) Zhang, C.; Li, L.; Zheng, S. Formation and Confined Crystallization of Polyethylene Nanophases in Epoxy Thermosets. *Macromolecules* **2013**, *46*, 2740–2753.
- (53) Ocando, C.; Fernández, R.; Tercjak, A.; Mondragon, I.; Eceiza, A. Nanostructured Thermoplastic Elastomers Based on SBS Triblock Copolymer Stiffening with Low Contents of Epoxy System. Morphological Behavior and Mechanical Properties. *Macromolecules* **2013**, *46*, 3444–3451.
- (54) Wang, L.; Li, J.; Li, L.; Zheng, S. Organic-inorganic Hybrid Diblock Copolymer Composed of Poly(ϵ -caprolactone) and Poly(MA POSS): Synthesis and Its Nanocomposites with Epoxy Resin. *J. Polym. Sci., Part A: Polym. Chem.* **2013**, *51*, 2079–2090.
- (55) Romeo, H. E.; Zucchi, I. A.; Rico, M.; Hoppe, C. E.; Williams, R. J. J. From Spherical Micelles to Hexagonally Packed Cylinders: The Cure Cycle Determines Nanostructures Generated in Block Copolymer/epoxy Blends. *Macromolecules* **2013**, *46*, 4854–4861.
- (56) Ruiz-Pérez, L.; Royston, G. J.; Fairclough, J. P. A.; Ryan, A. J. Toughening by Nanostructure. *Polymer* **2008**, *49*, 4475–4488.
- (57) Chieffari, J.; Mayadunne, R. T. A.; Moad, C. L.; Moad, G.; Rizzardo, E.; Postma, A.; Skidmore, M. A.; Thang, S. H. Thiocarbonylthio Compounds ($S=C(Z)S-R$) in Free Radical Polymerization with Reversible Addition-fragmentation Chain Transfer (RAFT) Polymerization. Effect of the Activating Group Z. *Macromolecules* **2003**, *36*, 2273–2283.
- (58) Thang, S. H.; Chong, B. Y. K.; Mayadunne, R. T. A.; Moad, G.; Rizzardo, E. A Novel Synthesis of Functional Dithioesters,

Dithiocarbamates, Xanthates and Trithiocarbonates. *Tetrahedron Lett.* **1999**, *40*, 2435–2438.

(59) Chong, B. Y. K.; Krstina, J.; Le, T. P. T.; Moad, G.; Postma, A.; Rizzardo, E.; Thang, S. H. Thiocarbonylthio Compounds [$S=C(Ph)S-R$] in Free Radical Polymerization with Reversible Addition-Fragmentation Chain Transfer (RAFT Polymerization). Role of the Free-radical Leaving Group (R). *Macromolecules* **2003**, *36*, 2256–2272.

(60) Robeson, L. M. The Effect of Antiplasticization on Secondary Loss Transitions and Permeability of Polymers. *Polym. Eng. Sci.* **1969**, *9*, 277–281.

(61) Jones, A. A. Molecular Level Model for Motion and Relaxation in Glassy Polycarbonate. *Macromolecules* **1985**, *18*, 902–906.

(62) Kim, B. S.; Mather, P. T. Amphiphilic Telechelics Incorporating Polyhedral Oligosilsesquioxane: 1. Synthesis and Characterization. *Macromolecules* **2002**, *35*, 8378–8384.

(63) Luo, X.; Zheng, S.; Zhang, N.; Ma, D. Miscibility of Epoxy Resins/poly(ethylene oxide) Blends Cured with Phthalic Anhydride. *Polymer* **1994**, *35*, 2619–2623.

(64) Zheng, S.; Zhang, N.; Luo, X.; Ma, D. Epoxy Resin/poly(ethylene oxide) Blends Cured with Aromatic Amine. *Polymer* **1995**, *36*, 3609–3613.

(65) Wagner, K. W. Erklärung Der Dielektrischen Nachwirkungsvorgänge Auf Grund Maxwellsscher Vorstellungen. *Arch. Elektrotech.* **1914**, *2*, 371–387.

(66) Sillars, R. W. The Properties of a Dielectric Containing Semiconducting Particles of Various Shapes. *J. Inst. Electr. Eng.* **1937**, *80*, 378–394.